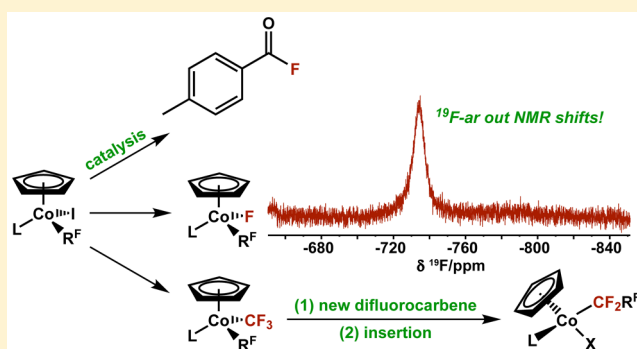


Perfluoroalkyl Cobalt(III) Fluoride and Bis(perfluoroalkyl) Complexes: Catalytic Fluorination and Selective Difluorocarbene Formation

Matthew C. Leclerc,[†] Julia M. Bayne,[†] Graham M. Lee,[†] Serge I. Gorelsky,[†] Monica Vasiliu,[‡] Ilia Korobkov,[†] Daniel J. Harrison,[†] David A. Dixon,[‡] and R. Tom Baker^{*,†}[†]Department of Chemistry and Biomolecular Sciences and Centre for Catalysis Research and Innovation, University of Ottawa, 30 Marie Curie, Ottawa, Ontario K1N 6N5, Canada[‡]Department of Chemistry, The University of Alabama, Tuscaloosa, Alabama 35487, United States

S Supporting Information

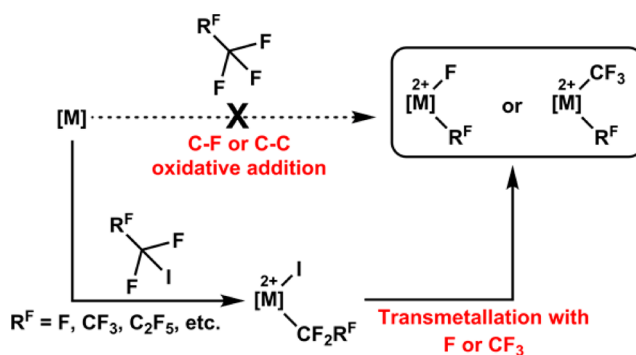
ABSTRACT: Four perfluoroalkyl cobalt(III) fluoride complexes have been synthesized and characterized by elemental analysis, multinuclear NMR spectroscopy, X-ray crystallography, and powder X-ray diffraction. The remarkable cobalt fluoride ¹⁹F NMR chemical shifts (−716 to −759 ppm) were studied computationally, and the contributing paramagnetic and diamagnetic factors were extracted. Additionally, the complexes were shown to be active in the catalytic fluorination of *p*-toluoyl chloride. Furthermore, two examples of cobalt(III) bis(perfluoroalkyl) complexes were synthesized and their reactivity studied. Interestingly, abstraction of a fluoride ion from these complexes led to selective formation of cobalt difluorocarbene complexes derived from the trifluoromethyl ligand. These electrophilic difluorocarbenes were shown to undergo insertion into the remaining perfluoroalkyl fragment, demonstrating the elongation of a perfluoroalkyl chain arising from a difluorocarbene insertion on a cobalt metal center. The reactions of both the fluoride and bis(perfluoroalkyl) complexes provide insight into the potential catalytic applications of these model systems to form small fluorinated molecules as well as fluoropolymers.



■ INTRODUCTION

Transition metal complexes bearing fluoride or fluorocarbon ligands have attracted considerable interest because they are used to mediate/catalyze C–F or C–R^F bond-forming reactions, which are highly important in the pharmaceutical, agrochemical, and advanced materials industries.^{1,2} Despite this widespread interest, the fundamental chemistry of these species is considerably less developed than that of analogous hydrocarbon compounds. In particular, reports of complexes bearing two fluorinated ligands (i.e., one perfluoroalkyl and one fluoride, or two perfluoroalkyls) are very rare, with most examples belonging to second or third row metals.³ Recently, examples of Ni complexes bearing two perfluoroalkyl ligands have been reported.⁴ There are synthetic challenges associated with preparing such complexes: The most direct approach would be via oxidative addition of the C–F or C–C bond of a perfluoroalkane (CF₄, C₂F₆, C₃F₈, etc.) to a low-valent metal, but the inert nature of perfluoroalkanes makes this route inaccessible.¹ Here, we use alternative synthetic routes to access the products of the hypothetical oxidative addition reaction between perfluoroalkanes and first row metals. Our general strategy is to utilize the oxidative addition of iodoperfluoroalkanes (R^F–I) to install the first perfluoroalkyl group on the metal, followed by exchange of the iodide ligand for either a fluoride or a trifluoromethyl group (Scheme 1). Oxidative

Scheme 1. Alternative Synthetic Route to Transition Metal Fluorides and Perfluoroalkyls

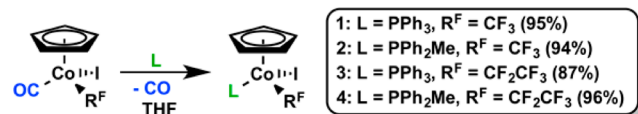


addition of R^F–I to metal complexes has been shown to proceed for group 9 metals,⁵ and methods for converting [M]–X (X = halide) to [M]–F⁶ or to [M]–CF₃^{2,7} are known. Reactions between the inexpensive and commercially available cobalt(I) complex CpCo(CO)₂ (Cp = η⁵-cyclopentadienyl) and R^F–I (R^F = CF₃ and CF₂CF₃) furnish cobalt(III)

Received: August 31, 2015

complexes $\text{CpCo}(\text{R}^{\text{F}})(\text{I})(\text{CO})$.⁸ Substitution of the carbonyl ligand with a phosphine is facile and leads to the series of isolable starting materials $\text{CpCo}(\text{R}^{\text{F}})(\text{I})(\text{L})$ (**1–4**), as shown in Scheme 2.⁹

Scheme 2. Synthetic Scheme for Phosphine Substitutions

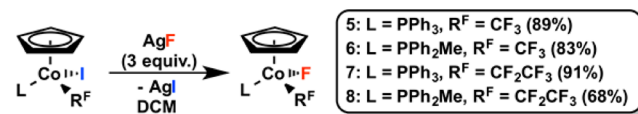


In recent reports, we described the two-electron reduction of complexes **1–4** with sodium to furnish a series of nucleophilic Co^{I} perfluorocarbene complexes, and demonstrated $[2 + 2]$ cycloaddition reactions with tetrafluoroethylene.¹⁰ The resulting cobalt(III) perfluorometallacyclobutane complexes reacted with both Lewis and Brønsted acids to give ring-opening/isomerization products. However, the chemistry of cobalt(III) systems with multiple perfluorinated ligands remains largely unexplored, and herein we expand that area.

RESULTS AND DISCUSSION

Synthesis and Characterization of Perfluoroalkyl Cobalt Fluorides. Seeking to isolate the hypothetical products that would arise from the oxidative addition of perfluoroalkanes to a cobalt center, we opted for a pathway involving the substitution of iodide for fluoride, using a method previously reported by Hughes et al. to afford analogous perfluoroalkyl Ir^{III} fluorides.^{6b} Reactions of complexes **1–4** with 3 equiv of AgF in dichloromethane at room temperature over 20 h in the absence of light afforded perfluoroalkyl Co^{III} fluoride complexes of the general formula $\text{CpCo}(\text{R}^{\text{F}})(\text{F})(\text{L})$ ($\text{Cp} = \eta^5\text{-cyclopentadienyl}$, $\text{R}^{\text{F}} = \text{CF}_3$ and CF_2CF_3 , $\text{L} = \text{PPh}_3$ and PPh_2Me) (**5–8**) in 68–91% isolated yield as dark-green solids (Scheme 3). Complexes

Scheme 3. Synthesis Scheme for Cobalt(III) Fluorides



5–8 were characterized spectroscopically and structurally, and the results were further analyzed by density functional theory (DFT)¹¹ calculations with the B3LYP^{12,13} and PW91^{14,15} exchange-correlation functionals and polarized double- and triple- ζ basis sets. Structurally, complexes **5** and **6** represent the expected products arising from the oxidative addition of perfluoromethane to cobalt, whereas complexes **7** and **8** are those that would arise from the same type of reaction with perfluoroethane. As previously mentioned, these oxidative addition reactions are not feasible; thus, it is necessary to utilize other synthetic methods to obtain such complexes.

Cobalt fluorides are uncommon in the literature, and the few that have been presented mostly feature cobalt in either the +1 or the +2 oxidation state.¹⁶ There are only three examples featuring cobalt in the +3 oxidation state: cobaltocenium fluoride, CoF_3 , and an example from Klein et al. with a cyclometalated complex featuring azine as an anchoring group.¹⁷ Cobaltocenium fluoride was synthesized by Richmond et al. in 1994,¹⁸ and has been applied to several stoichiometric fluorination reactions. This extremely hygroscopic reagent is

formed from the reaction of the one-electron reductant cobaltocene with an excess of perfluorodecalin in toluene at low temperature. CoF_3 is commercially available, although it is often too reactive to promote transformations in a selective manner. Of these three systems, only cobaltocenium fluoride and the cyclometalated cobalt fluoride are truly organometallic complexes, but they do not offer any opportunity for varying the ligand environment on cobalt because their scaffolds are limited as a result of the conditions of forming the fluorides, contrary to complexes **5–8**, which offer the ability to modify both the nature of the phosphine ligands and the perfluoroalkyl ligands on cobalt.

X-ray structural studies confirm that complexes **5–8** are well-defined monomeric Co^{III} fluorides featuring cyclopentadienyl, phosphine, and perfluoroalkyl ligands (Figure 1). The Co–F

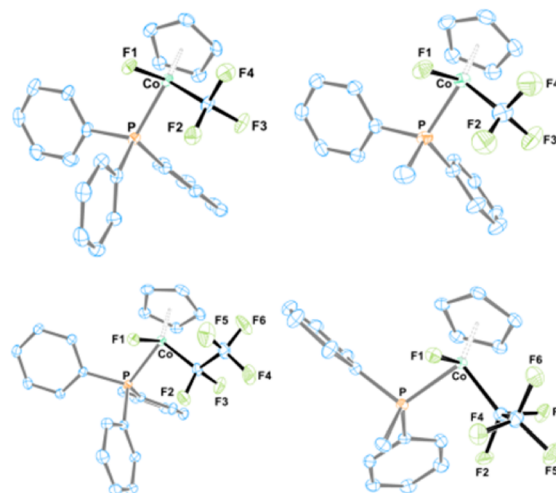


Figure 1. Crystallographic representations of **5** (top left), **6** (top right), **7** (bottom left), and **8** (bottom right) with 30% probability thermal ellipsoids. Hydrogen atoms are omitted for clarity. One molecule of acetonitrile has been removed from **5**. Sample of **6** crystallized with two molecules in the unit cell. Selected bond lengths and angles are presented in Table S1.

bond distances in complexes **5–8** range from 1.86 to 1.88 Å (Table S1), similar to the value of 1.89 Å found in CoF_3 .¹⁹ For perfluoroethyl complexes **7** and **8**, the $\text{C}_\alpha\text{–F}$ bond distances (avg. 1.378(2) and 1.393(2) Å) are significantly longer than $\text{C}_\beta\text{–F}$ (avg. 1.326(2) and 1.333(2) Å) as observed previously for an Ir analog.^{6b} The Co–P distances are approximately 0.04 Å shorter with PPh_2Me as compared to PPh_3 because the former is known to be a slightly more basic donor ligand. Moreover, the Co–C bond distances are shorter for the trifluoromethyl ligand versus the perfluoroethyl fragment by 0.2 Å for the PPh_3 derivatives and 0.4 Å for the PPh_2Me examples. Seminal work by Stone et al. has established that $[\text{M}]\text{–C}$ bonds are shorter with perfluoroalkyls than with analogous hydrocarbons, an effect observed in this system as well.²⁰ Recently, another example of a transition metal simultaneously bearing a fluoride and a perfluoroalkyl was reported that features a bis(trifluoromethyl) nickel dimer with bridging fluoride ligands.²¹

DFT calculations were used to gain insight into the electronic structure of **5** as a representative example. TD-DFT calculations at the B3LYP/TZVP level with the SMD solvent model²² reproduced the electronic absorption spectrum in CH_2Cl_2 well, with two principal experimental bands at 16

300 cm^{-1} (263 $\text{M}^{-1} \text{cm}^{-1}$, calcd = 15 600 cm^{-1}) and 21 800 cm^{-1} (1190 $\text{M}^{-1} \text{cm}^{-1}$, calcd = 21 700 cm^{-1}). (See Figure S1 and the band assignments in the [Supporting Information](#).) Relative to typical Co^{III} octahedral inorganic complexes,²³ the high intensities of these two absorption bands indicate significant charge-transfer character in the corresponding electron excitations. Calculated Mayer bond orders²⁴ for **5** provide values for Co–Cp (2.37), Co–PPh₃ (0.98), and Co–CF₃ bonds (0.91) that are unsurprising. However, the value for the Co–F bond (0.61) indicates significant ionic character in this metal–ligand interaction and that the Co–F is the least covalent among the metal–ligand bonds.

The ¹⁹F NMR spectra of **5**–**8** exhibit extreme upfield resonances for the fluoride ligands ranging from δ –716 to –759 ppm. These shifts are significantly upfield from the analogous Ir complexes previously reported by both Hughes et al.^{6b} ($\delta(^{19}\text{F})$ = –437 to –446 ppm) and Bergman et al.²⁵ ($\delta(^{19}\text{F})$ = –413 to –415 ppm). To the best of our knowledge, these represent the most upfield resonances reported for a ¹⁹F NMR signal. The resonances at half-height are very broad (900–1900 Hz) and featureless, presumably because of the fluorides being bound to ⁵⁹Co, a nuclide with a spin of $7/2$, a natural abundance of 100%, and a large quadrupolar coupling constant of $42.0 \times 10^{-30} \text{ m}^2$, all of which contribute to a significant broadening of the fluoride signal. The addition of molecular sieves to an NMR sample of **5**–**8** did not affect the broadness of the fluoride signals, indicating that the signal is not broadened artificially by the presence of moisture.

From the results of DFT computational studies, we are now able to understand the unique nature of these chemical shifts. The results for all of the calculated Co–F chemical shifts and their diamagnetic and paramagnetic tensor components are shown in the [Supporting Information](#). There are minor quantitative differences between the three sets of chemical calculations but not qualitative differences. There is reasonable agreement with experiment for the CF₃ and CF₂ chemical shifts with differences of up to 30 ppm, which is typical of such fluorine NMR calculations. The differences between the experimental and the calculated shifts for the F bonded to the Co are larger by 30–100 ppm depending on the method, with the BLYP/TZVP2 results being the closest to experiment for this shift. The magnitudes of the calculated shifts for the Co–F were found to be very sensitive to the bond distance, suggesting why the difference between the calculated and experimental values for this shift can be large. For L = PPh₃ and R = CF₃, the calculations predict a small value for the ¹⁹F shift of the CF₃ group (ca. –20 ppm as compared to the experimental value of –2 ppm), so the difference in the diamagnetic and paramagnetic components are comparable to those of the standard CFCl₃ (BLYP/TZ2P $\sigma(\text{standard})$ = 118.8 ppm) with the diamagnetic component larger than the paramagnetic component. The ¹⁹F chemical shift for the F bonded to the Co is large and negative, resulting from the fact that the diamagnetic and paramagnetic components have the same sign, both shielding. The paramagnetic component is larger than the diamagnetic component. We note that the diamagnetic shielding component for the F bonded to C and of the F bonded to Co are very similar, within ~10 ppm, so the large changes are due to the differences in the paramagnetic components between the “normal” value for the F in the CF₃ group and the value predicted for the F bonded to Co.

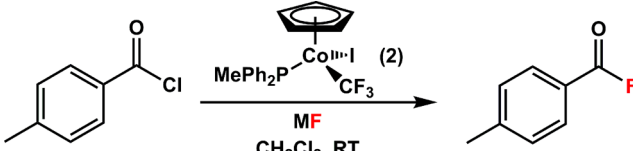
The fact that the paramagnetic component tensor has the same sign as the diamagnetic component tensor has been noted

previously for ClF because of mixing of the appropriate π orbitals with the σ^* orbital in the presence of a magnetic field.²⁶ Although F₂ has the same mixing interactions, the presence of symmetry prevents the paramagnetic component from being shielding. The high-lying occupied and low-lying unoccupied molecular orbitals (HOMO and LUMO, respectively) for CpCo(CF₃)(F)(PH₃) and CpCo(CF₃)(F)(PPh₃) are shown in the [Supporting Information](#). The orbitals are essentially the same for both compounds. The HOMO, HOMO-1, and HOMO-2 are lone pairs on the F bonded to Co interacting with different d orbitals on the Co. For the Co contribution, the HOMO is the $d_{x^2-y^2}$, the HOMO-1 is the d_{z^2} , and the HOMO-2 is the d_{xy} . The LUMO is the Co–F σ^* orbital with the d_{xz} on the Co, and the LUMO+1 is predominantly the Co–C σ^* . Thus, the HOMO, HOMO-1, and HOMO-2 serve as the equivalent to the π -type orbitals in ClF, and the LUMO is the equivalent of the ClF σ^* . It is the interaction of these orbitals in the presence of a magnetic field that leads to the paramagnetic component being shielding, similar to what is found for ClF.

Reactivity of Fluoride Complexes. The importance of fluorinated organic substrates has been amply demonstrated.²⁷ Efficient, reliable techniques for the introduction of fluorine into such products have been the subject of widespread research for many years.²⁸ Consequently, and encouraged by the ionic character of the Co–F bonds in our system, we sought to determine the ability of these cobalt systems to fluorinate simple organic compounds. Reactions with *p*-toluoyl chloride were explored as a potential route toward fluorination to form *p*-toluoyl fluoride. Gray et al. have recently demonstrated this reaction in stoichiometric fashion, proceeding through halide metathesis with cyclometalated iridium fluoride complexes.²⁹ Stoichiometric reactions with complex **6** in C₆D₆ showed clean and essentially complete conversion of the starting substrate within 2 h and formation of the *p*-toluoyl fluoride product, proceeding through overall halide metathesis with the cobalt fluoride complex. Prompted by the initial results of these stoichiometric reactions, we aimed to develop a catalytic process whereby, starting with the iodide complex **2**, the fluoride complex **6** could be generated in situ by the presence of an excess of AgF.

Control experiments convincingly demonstrated that stoichiometric reactions between *p*-toluoyl chloride and the fluoride sources AgF, CsF, KF, and CoF₃ gave minimal conversion of the starting reagent to the target compound overnight in dichloromethane (<5% in all cases). Optimized reaction conditions led to essentially quantitative conversion of the starting chloride to the fluoride within 4 h, using 5 mol % of **2** and 3 equiv of AgF. (See [Table 1](#) for selected control experiments and [Table S16](#) for a full list.) This catalytic fluorination occurs cleanly, affording an approximately 1:1 mixture of the Co–F and Co–Cl complexes upon completion. Relatively few methods of producing *p*-toluoyl fluoride exist in the literature, and they feature either exotic or potentially harmful reagents such as cyanuric fluoride,³⁰ cesium fluoroxysulfate,³¹ potassium bifluoride,³² and hydrogen fluoride.³³ Furthermore, this substrate is not commercially available, but Pd-based systems are used to produce it catalytically.³⁴ Two stoichiometric reactions were run in parallel, one of them containing excess PPh₂Me (5 equiv), and analyzed at the same time. Both reactions provided the same amount of conversion to the target product. It thus appears unlikely that the reaction proceeds through a dissociative mechanism, wherein the

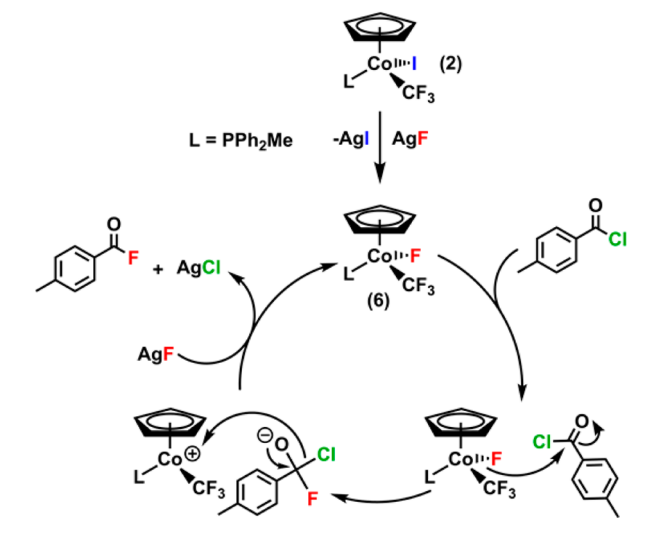
Table 1. Catalytic Fluorination Reactions



entry	MF (equiv)	catalyst loading (mol %)	t (h)	yield (%)
1	AgF (1.0)		16	2
2	CsF (1.0)		16	5
3	KF (1.0)		16	<1
4	CoF ₃ (1.0)		16	2
10	AgF (3.0)	10	4	99
14	AgF (3.0)	5	4	99
15	AgF (3.0)	1	4	47
16	AgF (3.0)	0.1	4	26

phosphine could dissociate from the metal and vacate a coordination site for the acyl chloride to bind.

With this information in hand, a proposed catalytic cycle is shown in Scheme 4. Starting from iodide complex 2, fluoride

Scheme 4. Proposed Catalytic Cycle for the Fluorination of *p*-Toluenoyl Chloride

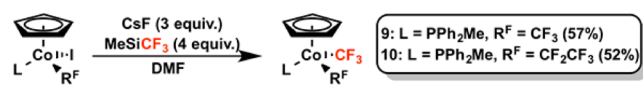
analogue 6 is first formed using AgF as the fluoride source. The ionic nature of the Co–F bond provides a latent source of fluoride, which can react readily with the electrophilic carbon center of the acyl chloride. Expulsion of the chloride from the organic substrate gives the target compound, generating a cobalt chloride complex, which can react with AgF to regenerate the catalytically active complex 6 and form the inactive AgCl. Many examples of electrophilic fluorination of organic substrates have been explored over recent years,³⁵ and efficient catalytic nucleophilic fluorination has more recently made major strides as well.³⁶ Importantly, transition metals have been used to perform the nucleophilic fluorination of a variety of alkyl fluorides,³⁷ alkenyl fluorides,³⁸ and aryl fluorides.³⁹ Alkyl fluorides have been synthesized by Toste et al. from gold(III)^{37a} systems and by Sanford et al. from palladium(IV)^{37c,39a} systems. Electrophilic gold(I)^{38a,b} complexes have been used almost exclusively for the synthesis of alkenyl fluorides, affording good yields and regioselectivity. Aryl fluorides have been synthesized by the groups of Sanford et al.

and Gagné et al. through the use of palladium(IV)^{39a} and platinum(IV),^{39b} respectively, as well as certain silver salts^{39c–e} and some copper complexes.⁴⁰ Additionally, Grushin et al. have reported various fluorination examples with palladium(II) and rhodium(I) systems.⁴¹ Of these examples, only copper stands out as a nonprecious, first row transition metal. Catalytic systems incorporating these types of abundant and nontoxic metals are very important and are active areas of research as the search for renewable and efficient methods of producing target fluorinated reagents continues. Moreover, the catalytic formation of C(sp²)–F bonds has mostly been limited to examples with palladium^{40b,42} as well as a few with copper^{40a} and gold.^{38a,b}

The tendency of third row transition metals to form weaker bonds to fluorine than most first row transition metals has made them useful for catalytic reactions,^{1,43} but it is essential to develop methods that utilize inexpensive, nontoxic, and abundant metals such as cobalt. Interestingly, it appears that the significant ionic character of the Co–F bond in this system, as demonstrated by the calculated Mayer bond orders, might be a major contributing factor to its catalytic potential. Furthermore, this reaction does not require the use of extravagant reagents and represents a step toward the potential uses of cobalt in additional catalytic fluorination reactions.

Synthesis and Characterization of Cobalt Bis(perfluoroalkyls). The isolation of perfluoroalkyl cobalt(III) halide complexes 1–8 motivated efforts to generate bis(perfluoroalkyl) complexes via transmetalation of the halide group with CF₃. Converting [M]–X complexes to [M]–CF₃ is an established process, first presented by Fuchikami et al.⁴⁴ using a copper system and Me₃SiCF₃ and subsequently by other groups.^{7c,d} We initiated our investigation by studying the reactivity of the Co^{III} perfluoroalkyl halide complexes with Me₃SiCF₃, using CsF as the initiator and DMF as solvent. Reactions with PPh₃ derivatives mostly resulted in decomposition and very low yields of the desired products. However, reactions with PPh₂Me derivatives (2, 4, 6, and 8) led to the desired bis(perfluoroalkyl) products (9 and 10) in good yields (9 = 71% and 10 = 75% from [Co]–F, 9 = 57% and 10 = 52% from [Co]–I) after only 2 h as stable yellow-orange powders (Scheme 5). Although the relative yields are lower when starting from [Co]–I complexes, it is an overall more direct approach to complexes 9 and 10.

Scheme 5. Synthesis Scheme for Cobalt(III) Bis(perfluoroalkyls)



It has been demonstrated previously that Me₃SiCF₃ undergoes activation by fluoride to liberate CF₃. Important studies by Yagupolskii et al.⁴⁵ and Röscenthaler et al.⁴⁶ independently demonstrated that this activation involves the in situ formation of pentacoordinate silicate anions, either [Me₃SiF(CF₃)][–] or [Me₃Si(CF₃)₂][–], which extrude [CF₃][–] to form Me₃SiF or Me₃SiCF₃, respectively. We propose that in our system, CsF reacts with Me₃SiCF₃ to produce the cesium salts of the aforementioned pentacoordinate silicates, which then effect the transmetalation with [Co]–X. This is in contrast to a report by Wang et al.,⁴⁷ where the reaction between AgF and Me₃SiCF₃ forms a proposed [AgCF₃] species that can effect trans-

metallation. It is important to note that for [Co]–I complexes **2** and **4**, CsI is formed during the course of the reaction. In addition, experiments in our lab show the following: (1) When CsI is used in the place of CsF, no transmetalation takes place. (2) [Co]–I complexes **2** and **4** do not react with CsF in DMF to produce [Co]–F complexes **6** and **8**. These observations are consistent with the lower yield of products **9/10** when starting from [Co]–I (**2/4**) rather than [Co]–F (**6/8**).

Complexes **9** and **10** were studied through X-ray crystallography (Figure 2). The Co–C bond distance of

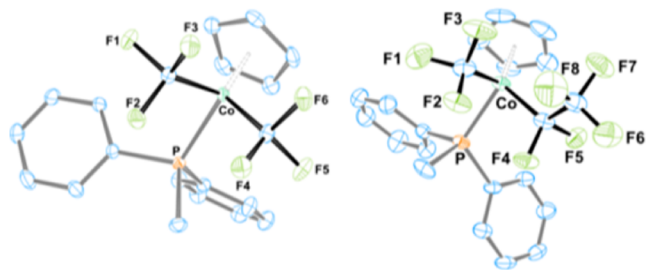


Figure 2. Crystallographic representations of **9** (left) and **10** (right) with 30% probability thermal ellipsoids. Hydrogen atoms are omitted for clarity. One molecule of toluene has been removed from both **9** and **10**. Selected bond lengths and angles are presented in Table S2.

1.940 Å in **9** is significantly longer than the Ni–C bond distances in analogous nickel bis(trifluoromethyl) complexes: The (bipy)Ni(CF₃)₂ complex from Vicić et al.^{4a} has a distance of 1.88 Å, and an example from Mirica et al.^{4b} has a distance of 1.91 Å with the Ni^{II} complex. However, the latter's bond lengths increase to 1.97 Å when the metal is oxidized to Ni^{III}. A recent report by Sanford et al. features an octahedral Ni^{IV} complex, TpNi(Ph)(CF₃)₂ (Tp = trispyrazolylborate), with Ni–C bond distances of 1.99 Å.^{4c} It is interesting to compare this complex with **9** because they are both d⁶ systems, and the Ni^{IV} complex was proven capable of promoting Aryl–CF₃ coupling through reductive elimination.

DFT calculations were used to obtain insight into the electronic structure of **9**. TD-DFT calculations at the B3LYP/TZVP level reproduce the electronic absorption spectrum well (Figure S1). The absorption bands in **9** are blue-shifted relative to the spectrum of **5**. The assignment of two bands at 23 000 cm^{−1} (shoulder) and 25 800 cm^{−1} (730 M^{−1} cm^{−1}) is shown in the Supporting Information. Calculated Mayer bond orders for **9** are 2.31 for the Co–Cp bond, 1.01 for Co–PPh₂Me, and 0.93 and 0.95 for the two Co–CF₃ bonds. These bond orders are almost identical to those in **5**. Thus, replacement of the fluoride ligand in **5** with the more strongly covalently bound CF₃ ligand does not affect the covalency of other Co–ligand interactions.

Full NMR characterization of these complexes was obtained, and assignment of the nonequivalent methylene fluorine resonances in the various ¹⁹F spectra was achieved. A 1D ¹H–¹⁹F HOESY experiment allowed the selective pulsing of each of the three different fluorine resonances to determine the relative spatial proximity to the three closest protons in the structure (Figure 3). Additionally, a ¹⁹F–¹⁹F NOESY was collected to observe how the trifluoromethyl ligand correlated through space to the different methylene fluorines of the perfluoroethyl ligand (Figure S34). These experiments indicate that the relative orientation of the ligands is essentially the same in solution as in the solid state.

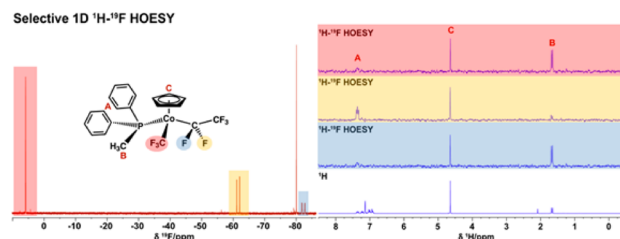


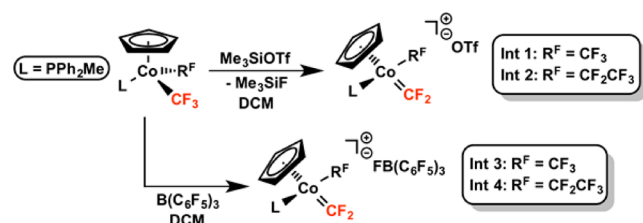
Figure 3. Selective 1D ¹H–¹⁹F HOESY experiment in C₆D₆ to help in the assignment of the two [Co]–CF₂CF₃ fluorine signals is shown. The Cp signals were set to equal intensity for the purposes of clarity. Colored boxes above the ¹H spectrum demonstrate the effect of selective saturation of the appropriate fluorine signal and showing which signals are correlated by a through-space interaction.

The 1D ¹H–¹⁹F HOESY experiment has been utilized recently by Claridge et al.⁴⁸ in the analysis of fluorinated pyrrolidines. This experiment offers the advantage of being much faster than the more prevalent 2D ¹⁹F–¹⁹F NOESY experiments found in the literature. In our case, by taking advantage of two nuclides in ¹H and ¹⁹F that each have essentially 100% natural abundance, the 1D method offers the possibility to obtain similar conformational information in a matter of minutes, as opposed to several hours for the traditional 2D method.

Reactivity of Bis(perfluoroalkyl) Complexes. Transition metal perfluoroalkyl complexes can be precursors to metal fluorocarbenes. We previously reported the two-electron reduction of perfluoroalkyl Co^{III} iodide complexes **1–4** to afford Co^I fluorocarbene complexes, which exhibit nucleophilic type reactivity at the carbene carbon.¹⁰ We are interested in preparing analogous Co^{III} fluorocarbenes in order to probe the effect that changing the oxidation state of cobalt will have on carbene reactivity, with the expectation that Co^{III} fluorocarbenes might react as electrophiles. This concept was previously demonstrated in an elegant study by Roper et al., where they showed that Ru⁰ and Ru^{II} fluorocarbenes differed by having nucleophilic and electrophilic reactivity at the carbene carbon, respectively.⁴⁹

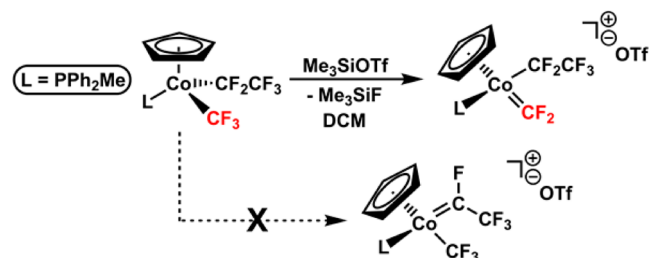
Our strategy to prepare Co^{III} fluorocarbenes consisted of abstracting a fluoride from a perfluoroalkyl ligand using a Lewis acid, similar to the preparation of other fluorocarbene complexes in the literature. Our initial attempts to abstract a fluoride from perfluoroalkyl Co^{III} iodides **1–4** were unsuccessful because reactions with the Lewis acids Me₃SiOTf and B(C₆F₅)₃ did not result in the formation of fluorocarbenes, presumably as a result of a preference by the Lewis acid to abstract the iodide ligand. However, bis(perfluoroalkyl) complexes **9–10** were attractive precursors for fluorocarbene formation because they both eliminate the possibility of an undesirable metal halide abstraction. Indeed, reactions of **9** and **10** with Lewis acids (Me₃SiOTf and B(C₆F₅)₃) in DCM led to fluoride abstraction and formation of cobalt difluorocarbene complexes (Int **1–4**, Scheme 6). Addition of the Lewis acid to a solution of the bis(perfluoroalkyl) precursors led to a color change from yellow-orange to deep red over the course of 1 h at room temperature, and NMR analysis demonstrated that quantitative conversion was achieved. The ¹⁹F NMR resonances for the difluorocarbene ligand in complexes Int **1–4** are highly characteristic, with downfield chemical shifts ranging between δ 178 and 180 ppm.⁵⁰ This is in contrast to the difluorocarbene ligand of previously reported Co^I complexes, with resonances for the two unique fluorine environments at δ 63 and 94 ppm.¹⁰

Scheme 6. Formation of Cobalt(III) Difluorocarbenes



Both Lewis acids provided selective fluoride abstraction from complex **10** because only abstraction from the trifluoromethyl ligand was observed, leaving the perfluoroethyl fragment untouched (Scheme 7). This is supported by ^{19}F NMR,

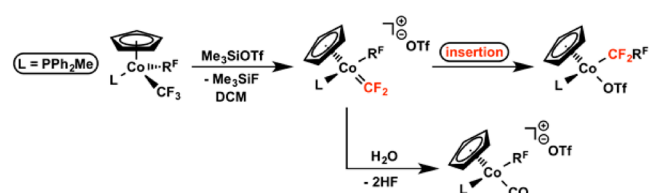
Scheme 7. Selectivity of Fluoride Abstraction



where the only fluorocarbene signal that is observed is the one associated with the difluorocarbene fragment and not that of the fluoro(trifluoromethyl) carbene. The selectivity of fluoride abstraction from CF_3 and not CF_2CF_3 can be rationalized by comparing the π -donating ability of F and CF_3 fragments. Metal carbene bonds are typically stabilized by contributions of d orbital electrons from the metal. However, because the Co^{III} carbene complexes here have two fewer d electrons compared to the Co^{I} carbenes we reported previously (d^6 vs d^8), the $\text{M}=\text{C}$ bond is likely more reliant on donation from the other carbene substituents for stabilization. Therefore, because F is a better π -donating substituent than CF_3 , fluoride abstraction from CF_3 rather than CF_2CF_3 is preferred. Efforts to increase electron density around the metal by utilizing PMe_3 in the hopes of promoting some amount of fluoride abstraction from the perfluoroethyl ligand were unsuccessful.

The newly formed difluorocarbene complexes underwent two primary reactions in solution, which prevented their isolation in pure form. One involves the insertion of difluorocarbene into the remaining perfluoroalkyl fragment, effectively increasing the length of the perfluoroalkyl chain on the transition metal center by one CF_2 unit (Scheme 8, top). These products are clearly identified using ^{19}F NMR because the resulting perfluoroethyl and perfluoropropyl ligands have highly characteristic chemical shifts and splitting patterns, which are identical to those of previously isolated Co^{III}

Scheme 8. Reactivity of Cobalt(III) Difluorocarbenes



complexes.⁵¹ Previous work by Burton et al.⁵² on copper demonstrated a rare example of this type of perfluoroalkyl chain growth from CF_2 insertion on a transition metal. This reaction demonstrates a step toward potential perfluoroalkene polymerization using a transition metal catalyst, a sought-after process that has been stunted at least in part by the difficulties involved in promoting such insertion reactions,⁵³ in large part due to the strength of various $[\text{M}]-\text{R}^{\text{F}}$ bonds. Attaining better control of this reaction is an area of ongoing study within our group.

The second reaction is the well-known hydrolysis of the difluorocarbene ligand by trace H_2O to furnish a carbonyl ligand and 2 equiv of HF (Scheme 8, bottom).⁵⁴ This reaction occurs almost instantaneously and is a common reaction with metal difluorocarbenes that have formal d^6 metal centers.^{49,55} Although the hydrolysis of difluorocarbene ligands is undesirable, the observation of electrophilic reactivity by our Co^{III} fluorocarbenes further highlights a key difference from our previously reported Co^{I} fluorocarbenes, which did not react with 20 equiv of H_2O in acetonitrile solutions.

CONCLUSIONS

We have isolated and characterized four perfluoroalkyl Co^{III} fluoride complexes. These complexes exhibit remarkable ^{19}F NMR shifts, largely due to an unusual paramagnetic component that is shielding. Additionally, these complexes were shown to be active in the catalytic fluorination of *p*-toluoyl chloride. Furthermore, both the fluoride and iodide complexes could be used in the synthesis of Co^{III} bis(perfluoroalkyl) complexes, potential precursors in the development of catalytically relevant systems. These complexes were shown to react with different Lewis acids to form electrophilic Co^{III} difluorocarbenes. The insertion of these difluorocarbenes into the remaining perfluoroalkyl fragment on the metal demonstrated the elongation of a perfluoroalkyl chain on a transition metal by one carbon. Further studies on the catalytic activity of these complexes are currently underway in our laboratory.

EXPERIMENTAL SECTION

General Considerations. All manipulations were carried out using standard Schlenk techniques or in an MBraun glovebox. All glassware was oven-dried at $>150^\circ\text{C}$ for a minimum of 2 h prior to use or flame-dried using a torch. Toluene, hexanes, tetrahydrofuran (THF), diethyl ether (DEE), and dimethylformamide (DMF) were dried on columns of activated alumina using a J. C. Meyer (formerly Glass Contour) solvent purification system. Dichloromethane (DCM), chloroform-*d* (CDCl_3), and acetonitrile- d_3 (CD_3CN) were dried by refluxing over calcium hydride under a nitrogen flow, followed by distillation and filtration through a column of activated alumina (ca. 10 wt %). Benzene- d_6 (C_6D_6) was dried by standing over activated alumina (ca. 10 wt %) overnight followed by filtration. The following chemicals were used as purchased, without further purification: $\text{CpCo}(\text{CO})_2$ ($\text{Cp} = \eta^5\text{-cyclopentadienyl}$) (Strem, 95%), CF_3I (SynQuest, 99%), $\text{CF}_3\text{CF}_2\text{I}$ (SynQuest, 98%), PPh_3 (Strem, 99%), PPh_2Me (Strem, 99%), Me_3SiOTf ($\text{OTf} = \text{SO}_3\text{CF}_3$) (Aldrich, 98%), AgF (Strem, 98%), CsF (Strem, 99+%), KF (Aldrich 99+%), CoF_3 (Aldrich, 98%), and *p*-toluoyl chloride (Aldrich, 98%). Starting complexes $\text{CpCo}(\text{R}^{\text{F}})(\text{I})(\text{CO})$ ($\text{Cp} = \eta^5\text{-cyclopentadienyl}$; $\text{R}^{\text{F}} = \text{CF}_3$ and CF_2CF_3) were synthesized according to slightly modified literature procedures from $\text{CpCo}(\text{CO})_2$.⁵ From these complexes, facile substitution of the CO ligands provided the phosphine analogues according to a slightly modified literature procedure.⁶ (See the Supporting Information for complete details on isolation of these complexes.) ^1H , ^{19}F , $^{19}\text{F}\{^1\text{H}\}$, and $^{31}\text{P}\{^1\text{H}\}$ NMR spectra were recorded on either a 300 MHz Bruker Avance or 300 MHz Bruker Avance II spectrometer at room temperature. ^1H NMR spectra were referenced to the residual proton

peaks associated with the deuterated solvents ($C_6D_6 = 7.16$ ppm, $CDCl_3 = 7.26$ ppm, $CD_3CN = 1.94$ ppm). ^{19}F and $^{19}F\{^1H\}$ NMR spectra were referenced to internal 1,3-bis(trifluoromethyl)benzene (BTB) (Aldrich, 99%, deoxygenated by purging with nitrogen and stored over 4 Å molecular sieves), set to -63.5 ppm. $^{31}P\{^1H\}$ NMR spectra were referenced to external H_3PO_4 (85% aqueous solution), set to 0.0 ppm. The ^{19}F NMR signals corresponding to the different $[Co]-CF_2CF_3$ complexes are labeled as A and A'. For labeling information, see Figure S24. Assignments were derived from 2D experiments with $CpCo(CF_2CF_3)(CF_3)(PPh_2Me)$ and applied to the other complexes because instrumental constraints did not permit the same experiments to be undertaken with the various fluoride complexes. Throughout this manuscript, F^A refers to the more upfield resonance and $F^{A'}$ refers to the more downfield resonance. UV-vis spectra were recorded on a Cary 100 instrument, using sealable quartz cuvettes (1.0 cm path length). Elemental analyses were performed by the Laboratoire d'Analyse Élémentaire de l'Université de Montréal (Montréal, Québec, Canada) and the G. G. Hatch Stable Isotope Laboratory at the University of Ottawa (Ottawa, Ontario, Canada). A Micromass Q-ToF 1 (positive mode) was used for electrospray ionization (ESI), with samples diluted to ca. 5 $\mu g/mL$ in methanol. Infrared spectroscopy was carried out on a Thermo Nicolet NEXUS 670 FTIR instrument. Powder X-ray diffraction (PXRD) experiments were performed using a RIGAKU Ultima IV, equipped with a Cu K α radiation source ($\lambda = 1.541836$ Å), and a graphite monochromator. Scanning of the 2θ range was performed from 5 to 40°. PXRD pattern was consistent in 2θ values with the generated pattern from XRD, with slight discrepancies in some intensities of peaks attributed to preferred crystallite orientation.

General Procedure for the Synthesis of $CpCo(R^F)(F)(L)$ ($R^F = CF_3$ or CF_2CF_3 ; $L = PPh_3$ or PPh_2Me). A 100 mL round-bottomed Schlenk flask was charged with $CpCo(R^F)(I)(L)$ (0.58 mmol) dissolved in CH_2Cl_2 (ca. 15 mL). AgF (1.74 mmol) was added, and the resulting solution/suspension was stirred at room temperature for approximately 20 h in the absence of light. After this time, a color change to dark green was observed. The resulting mixture was filtered through a plug of Celite, and the volatiles were removed in vacuo. The crude product was recrystallized from a concentrated solution of CH_2Cl_2 and hexanes at -35 °C. Pure product was collected via filtration, washed with cold (-35 °C) hexanes, and dried in vacuo. The products were obtained as dark-green powders. Crystals suitable for X-ray crystallography were obtained by diffusion of hexanes into a concentrated solution of the appropriate complex in toluene. Complexes 5 and 7 were not viable for elemental analysis (approximately 1–2% off) because we suspect a small amount of unidentified paramagnetic impurity. The latter also potentially contributes to the broadness of the 1H NMR spectra for these complexes. The use of various solvents and variable temperature NMR were unsuccessful in diminishing the broadening. Sublimation, additional recrystallizations, and column chromatography were attempted to try and purify these complexes. Column chromatography with a solvent mixture of THF/MeOH (8:2), followed by recrystallization from a concentrated solution of toluene proved most effective, but a small amount of impurity was retained. Additionally, THF inserts within the crystal lattice and cannot be removed under high vacuum (ca. 10^{-3} mtorr), even with heating. As such, PXRD patterns were compared with the calculated pattern from XRD in order to confirm the bulk-phase purity of complex 7 (Figure S37). The patterns were in excellent agreement with one another, thus confirming the crystalline-phase purity of the sample. The same comparison with complex 5 was unsuccessful because of the presence of solvent within the unit cell of the crystallographic data.

$CpCo(CF_3)(F)(PPh_3)$ (5). Yield: 245 mg, 89% based on $CpCo(CF_3)(I)(PPh_3)$. UV-vis (1.0 mM in CH_2Cl_2) $\lambda_{max}(\epsilon) = 459$ (1190), 615 (263). 1H NMR (300 MHz, C_6D_6) δ 4.60 (s, 5H, Cp), 6.98 (m, 6H, *m*- and *p*-CH(PPh)), 7.89 (m, 4H, *o*-CH(PPh)). ^{19}F NMR (282 MHz, C_6D_6) δ -2.0 (d, $^3J_{FF} \approx 8$ Hz, 3F, CF_3), -734 (br, $\omega_{1/2} \approx 1900$ Hz, 1F, Co-F). $^{31}P\{^1H\}$ NMR (121 MHz, C_6D_6) δ 29.8 (br, $\omega_{1/2} \approx 65$ Hz). Elemental analysis for $C_{24}H_{20}F_4PCo$ Calcd: C, 60.77; H, 4.25. Found: C, 58.73; H, 4.36.

$CpCo(CF_3)(F)(PPh_2Me)$ (6). Yield: 198 mg, 83% based on $CpCo(CF_3)(I)(PPh_2Me)$. UV-vis (0.5 mM in CH_2Cl_2) $\lambda_{max}(\epsilon) = 450$ (1640), 604 (347). 1H NMR (300 MHz, C_6D_6) δ 1.57 (d, $^2J_{HP} \approx 13$ Hz, 3H, CH_3), 4.60 (s, 5H, Cp), 7.05 (m, 6H, *m*- and *p*-CH(PPh)), 7.52 (dt, $^3J_{HH} \approx 8$ Hz, $^3J_{HP} \approx 78$ Hz, 4H, *o*-CH(PPh)). ^{19}F NMR (282 MHz, C_6D_6) δ -3.3 (d, $^3J_{FF} \approx 9$ Hz, 3F, CF_3), -716 (br, $\omega_{1/2} \approx 1300$ Hz, 1F, Co-F). $^{31}P\{^1H\}$ NMR (121 MHz, C_6D_6) δ 33.7 (br, $\omega_{1/2} \approx 130$ Hz). Elemental analysis for $C_{19}H_{18}F_4PCo$ Calcd: C, 55.36; H, 4.40. Found: C, 54.98; H, 4.69.

$CpCo(CF_2CF_3)(F)(PPh_3)$ (7). Yield: 277 mg, 91% based on $CpCo(CF_2CF_3)(I)(PPh_3)$. UV-vis (0.5 mM in CH_2Cl_2) $\lambda_{max}(\epsilon) = 473$ (1420), 621 (340). 1H NMR (300 MHz, $CDCl_3$) δ 4.61 (s, 5H, Cp), 7.40 (m, 6H, *m*- and *p*-CH(PPh)), 7.79 (m, 4H, *o*-CH(PPh)). ^{19}F NMR (282 MHz, $CDCl_3$) δ -68.6 (d, $^2J_{FF} \approx 240$ Hz, 1F, CF^AF^A ; F^A), -79.8 (d, $^4J_{FF} \approx 10$ Hz, 3F, CF_3), -81.0 (ddd, $^3J_{FF} \approx 46$ Hz, 1F, CF^AF^A ; F^A), -759 (br, $\omega_{1/2} \approx 1000$ Hz, 1F, Co-F). $^{31}P\{^1H\}$ NMR (121 MHz, $CDCl_3$) δ 26.3 (br, $\omega_{1/2} \approx 95$ Hz). Elemental analysis for $C_{25}H_{20}F_6PCo$ Calcd: C, 57.27; H, 3.84. Found: C, 55.93; H, 3.97.

$CpCo(CF_2CF_3)(F)(PPh_2Me)$ (8). Yield: 268 mg, 68% based on $CpCo(CF_2CF_3)(I)(PPh_2Me)$. UV-vis (0.25 mM in CH_2Cl_2) $\lambda_{max}(\epsilon) = 461$ (3140), 605 (680). 1H NMR (300 MHz, C_6D_6) δ 1.51 (d, $^2J_{HP} \approx 13$ Hz, 3H, CH_3), 4.60 (s, 5H, Cp), 7.07 (m, 6H, *m*- and *p*-CH(PPh)), 7.45 (dt, $^3J_{HH} \approx 7$ Hz, $^3J_{HP} \approx 55$ Hz, 4H, *o*-CH(PPh)). ^{19}F NMR (282 MHz, C_6D_6) δ -70.8 (d, $^2J_{FF} \approx 248$ Hz, 1F, CF^AF^A ; F^A), -79.7 (d, $^4J_{FF} \approx 12$ Hz, 3F, CF_3), -80.7 (dd, $^3J_{FF} \approx 43$ Hz, 1F, CF^AF^A ; F^A), -734 (br, $\omega_{1/2} \approx 900$ Hz, 1F, Co-F). $^{31}P\{^1H\}$ NMR (121 MHz, C_6D_6) δ 31.9 (br, $\omega_{1/2} \approx 130$ Hz). Elemental analysis for $C_{20}H_{18}F_6PCo$ Calcd: C, 51.97; H, 3.93. Found: C, 51.45; H, 4.06.

General Procedure for the Synthesis of $CpCo(R^F)(CF_3)(PPh_2Me)$ ($R^F = CF_3$ or CF_2CF_3). $CpCo(R^F)(I)(PPh_2Me)$ (0.877 mmol) was dissolved in DMF (15 mL), and CsF (2.63 mmol) was added as a solid. The resulting solution was stirred at room temperature for 5 min. To this solution was added dropwise Me_3SiCF_3 (4.22 mmol) in toluene (5 mL) over 3 min, and the reaction was stirred at room temperature for approximately 3 h. During this time, the color of the reaction mixture changed from dark green to bright orange. The mixture was then filtered through a pad of Celite, washed with ~ 10 mL of toluene, and the filtrate was evaporated under vacuum to dryness. The resulting residue was triturated with DEE (4 \times 10 mL). The orange solid was dissolved in minimal toluene and mounted on a silica-gel column. DEE was used as the eluent and pushed through the column until the washings were clear. The solvent was again removed under vacuum to afford pure product as a yellow-orange powder. Crystals suitable for X-ray crystallography were obtained from a concentrated solution of the appropriate complex in toluene cooled to -35 °C.

$CpCo(CF_3)_2(PPh_2Me)$ (9). Yield: 231 mg, 57% based on $CpCo(CF_3)(I)(PPh_2Me)$. UV-vis (0.5 mM in CH_2Cl_2) $\lambda_{max}(\epsilon) = 388$ (1335), 430 (shoulder of the principal band). 1H NMR (300 MHz, C_6D_6) δ 1.70 (d, $^2J_{HP} \approx 11$ Hz, 3H, CH_3), 4.63 (s, 5H, Cp), 7.01 (m, 6H, *m*- and *p*-CH(PPh)), 7.34 (m, 4H, *o*-CH(PPh)). ^{19}F NMR (282 MHz, C_6D_6) δ 3.6 (d, $^3J_{FF} \approx 3$ Hz, 6F, CF_3). $^{31}P\{^1H\}$ NMR (121 MHz, C_6D_6) δ 40.3 (br, $\omega_{1/2} \approx 150$ Hz). Elemental analysis for $C_{20}H_{18}F_6PCo$ Calcd: C, 51.97; H, 3.93. Found: C, 51.83; H, 3.99.

$CpCo(CF_2CF_3)(CF_3)(PPh_2Me)$ (10). Yield: 235 mg, 52% based on $CpCo(CF_2CF_3)(I)(PPh_2Me)$. UV-vis (0.75 mM in CH_2Cl_2) $\lambda_{max}(\epsilon) = 375$ (730), 450 (shoulder of the principal band). 1H NMR (300 MHz, CD_3CN) δ 1.69 (d, $^2J_{HP} \approx 11$ Hz, 3H, CH_3), 4.67 (s, 5H, Cp), 6.99 (m, 6H, *m*- and *p*-CH(PPh)), 7.31 (dt, $^3J_{HH} \approx 9$ Hz, $^3J_{HP} \approx 40$ Hz, 4H, *o*-CH(PPh)). ^{19}F NMR (282 MHz, CD_3CN) δ 5.2 (m, 3F, Co- CF_3), -62.3 (dd, $^2J_{FF} \approx 258$ Hz, $^3J_{FF} \approx 16$ Hz, 1F, CF^AF^A ; F^A), -80.7 (m, 3F, Co- CF_2CF_3), -82.9 (dm, $^2J_{FF} \approx 258$ Hz, 1F, CF^AF^A ; F^A). $^{31}P\{^1H\}$ NMR (121 MHz, CD_3CN) δ 37.2 (br, $\omega_{1/2} \approx 140$ Hz). Elemental analysis for $C_{21}H_{18}F_8PCo$ Calcd: C, 49.24; H, 3.54. Found: C, 49.16; H, 3.70.

General Procedure for the Determination of NMR Yields in the Formation of $[CpCo(R^F)(=CF_2)(PPh_2Me)](X)$ ($R^F = CF_3$ or CF_2CF_3 ; $X = OTf^-$ or $[FB(C_6F_5)_3]^-$) and the Products Derived from These Intermediates. Note that as the difluorocarbene

complexes form they react either with any trace quantities of water present (immediately) or in an insertion reaction (over a period of several hours). Furthermore, the reactions involving the difluorocarbene intermediates occur more quickly when using Me_3SiOTf as compared to $\text{B}(\text{C}_6\text{F}_5)_3$. Because of the enhanced stability of the difluorocarbenes formed by using $\text{B}(\text{C}_6\text{F}_5)_3$, yields for these complexes are reported for a certain reaction time. Because of the nature of these reactions, yields for the products deriving from the reactions with water and the insertion reactions will be presented for an elapsed reaction time with Me_3SiOTf and when possible with $\text{B}(\text{C}_6\text{F}_5)_3$.

Method A. $\text{CpCo}(\text{R}^f)(\text{CF}_3)(\text{PPh}_2\text{Me})$ (0.043 mmol) was dissolved in DCM (0.8 mL), and BTB (0.043 mmol) was added. The solution was transferred to an NMR tube, and Me_3SiOTf (0.043 mmol) was added with a microliter syringe. The NMR tube was sealed and shaken vigorously. The ^{19}F NMR yields were determined by integration of signals with respect to BTB. Complete conversion of starting material was observed within 60 min.

Method B. $\text{CpCo}(\text{R}^f)(\text{CF}_3)(\text{PPh}_2\text{Me})$ (0.043 mmol) was dissolved in DCM (0.4 mL), and BTB (0.043 mmol) was added. The solution was transferred to an NMR tube, and a solution of $\text{B}(\text{C}_6\text{F}_5)_3$ (0.043 mmol) in DCM (0.4 mL) was added. The NMR tube was sealed and shaken vigorously. The ^{19}F NMR yields were determined by integration of signals with respect to BTB. Complete conversion of starting material was observed within 30 min.

$[\text{CpCo}(\text{CF}_3)(=\text{CF}_2)(\text{PPh}_2\text{Me})][\text{OTf}]$ (**Int 1**). ^{19}F NMR (282 MHz, CH_2Cl_2 with C_6D_6 capillary) δ 180.0 (br, 2F, $\text{Co}=\text{CF}_2$), 9.0 (br, $\text{Co}-\text{CF}_3$), -78.9 (br, 3F, CF_3SO_3^-). $^{31}\text{P}\{^1\text{H}\}$ NMR (121 MHz, CH_2Cl_2 with C_6D_6 capillary) δ 40.1 (br, $\omega_{1/2} \approx 136$ Hz).

$[\text{CpCo}(\text{CF}_2\text{CF}_3)(=\text{CF}_2)(\text{PPh}_2\text{Me})][\text{OTf}]$ (**Int 2**). Yield: 68% based on $\text{Co}=\text{CF}_2$ after 30 min (20% after 4 h). ^{19}F NMR (282 MHz, CH_2Cl_2 with C_6D_6 capillary) δ 179.5 (br, 2F, $\text{Co}=\text{CF}_2$), -58.4 (d, $^2J_{\text{FF}} \approx 228$ Hz, 1F, $\text{CF}^{\text{A}}\text{F}^{\text{A}'}; \text{F}^{\text{A}}$), -75.3 (dd, $^2J_{\text{FF}} \approx 228$ Hz, $^3J_{\text{FF}} \approx 36$ Hz 1F, $\text{CF}^{\text{A}}\text{F}^{\text{A}'}; \text{F}^{\text{A}}$), -80.9 (br, 3F, $\text{Co}-\text{CF}_2\text{CF}_3$). $^{31}\text{P}\{^1\text{H}\}$ NMR (121 MHz, CH_2Cl_2 with C_6D_6 capillary) δ 35.6 (br, $\omega_{1/2} \approx 142$ Hz).

$[\text{CpCo}(\text{CF}_3)(=\text{CF}_2)(\text{PPh}_2\text{Me})][\text{FB}(\text{C}_6\text{F}_5)_3]$ (**Int 3**). ^{19}F NMR (282 MHz, CH_2Cl_2 with C_6D_6 capillary) δ 178.8 (br, 2F, $\text{Co}=\text{CF}_2$), 9.4 (br, $\text{Co}-\text{CF}_3$), -134.4 (d, br, $^3J_{\text{FF}} \approx 18$ Hz, 6F, $\text{FB}(\text{o}-\text{C}_6\text{F}_5)_3$), -159.1 (s, br, 3F, $\text{FB}(\text{o}-\text{C}_6\text{F}_5)_3$), -165.8 (m, br, 6F, $\text{FB}(\text{m}-\text{C}_6\text{F}_5)_3$), -188.8 (s, br, 1F, $\text{FB}(\text{C}_6\text{F}_5)_3$). $^{31}\text{P}\{^1\text{H}\}$ NMR (121 MHz, CH_2Cl_2 with C_6D_6 capillary) δ 37.6 (br, $\omega_{1/2} \approx 136$ Hz).

$[\text{CpCo}(\text{CF}_2\text{CF}_3)(=\text{CF}_2)(\text{PPh}_2\text{Me})][\text{FB}(\text{C}_6\text{F}_5)_3]$ (**Int 4**). Yield: 75% based on $\text{Co}=\text{CF}_2$ after 30 min (60% after 4 h). ^{19}F NMR (282 MHz, CH_2Cl_2 with C_6D_6 capillary) δ 178.2 (t, br, $^4J_{\text{FF}} \approx 7$ Hz, 2F, $\text{Co}=\text{CF}_2$), -57.2 (dm, $^2J_{\text{FF}} \approx 225$ Hz, 1F, $\text{CF}^{\text{A}}\text{F}^{\text{A}'}; \text{F}^{\text{A}}$), -74.6 (dd, $^2J_{\text{FF}} \approx 225$ Hz, $^3J_{\text{FF}} \approx 35$ Hz 1F, $\text{CF}^{\text{A}}\text{F}^{\text{A}'}; \text{F}^{\text{A}}$), -80.8 (br, 3F, $\text{Co}-\text{CF}_2\text{CF}_3$), -189.0 (s, br, 1F, $\text{FB}(\text{C}_6\text{F}_5)_3$). $^{31}\text{P}\{^1\text{H}\}$ NMR (121 MHz, CH_2Cl_2 with C_6D_6 capillary) δ 37.5 (br, $\omega_{1/2} \approx 148$ Hz).

Analysis of the Proposed Products Derived from Int 1–4 by ^{19}F NMR and Mass Spectrometry. $[\text{CpCo}(\text{CF}_3)(\text{CO})(\text{PPh}_2\text{Me})][\text{OTf}]$ (**from Int 1**). Yield: 14% based on $\text{Co}-\text{CF}_3$ after 60 min. ^{19}F NMR (282 MHz, CH_2Cl_2 with C_6D_6 capillary) δ 2.79 (br, 3F, $\text{Co}-\text{CF}_3$), -78.3 (br, 3F, CF_3SO_3^-). $^{31}\text{P}\{^1\text{H}\}$ NMR (121 MHz, CH_2Cl_2 with C_6D_6 capillary) δ 35.8 (br, $\omega_{1/2} \approx 75$ Hz). IR: 2241 cm^{-1} (s, br, $\text{Co}-\text{CO}$).

$\text{CpCo}(\text{CF}_2\text{CF}_3)(\text{OTf})(\text{PPh}_2\text{Me})$ (**from Int 1**). Yield: 18% based on $\text{Co}-\text{CF}_2\text{CF}_3$ after 60 min. ^{19}F NMR (282 MHz, CH_2Cl_2 with C_6D_6 capillary) δ -74.7 (dm, $^2J_{\text{FF}} \approx 247$ Hz, 1F, $\text{CF}^{\text{A}}\text{F}^{\text{A}'}; \text{F}^{\text{A}}$), -78.1 (br, 3F, CF_3SO_3^-), -80.3 (br, 3F, $\text{Co}-\text{CF}_2\text{CF}_3$), -83.9 (dd, $^2J_{\text{FF}} \approx 247$ Hz, $^3J_{\text{FF}} \approx 30$ Hz 1F, $\text{CF}^{\text{A}}\text{F}^{\text{A}'}; \text{F}^{\text{A}}$). $^{31}\text{P}\{^1\text{H}\}$ NMR (121 MHz, CH_2Cl_2 with C_6D_6 capillary) δ 30.0 (br, $\omega_{1/2} \approx 97$ Hz). MS [ESI (positive mode), solvent: MeOH] Calcd m/z (% intensity) for $[\text{CpCo}(\text{CF}_2\text{CF}_3)(\text{PPh}_2\text{Me})]^+$ 443.04 (100), 444.04 (22), 445.05 (2). Found: 443.04 (100), 444.04 (23).

$[\text{CpCo}(\text{CF}_2\text{CF}_3)(\text{CO})(\text{PPh}_2\text{Me})][\text{OTf}]$ (**from Int 2**). Yield and NMR assignments could not be obtained because of peak overlap. IR: 2243 cm^{-1} (s, br, $\text{Co}-\text{CO}$).

$\text{CpCo}(\text{CF}_2\text{CF}_2\text{CF}_3)(\text{OTf})(\text{PPh}_2\text{Me})$ (**from Int 2**). Yield: 13% based on $\text{Co}-\text{CF}_2\text{CF}_2\text{CF}_3$ after 4 h. Only the F_β signals of the perfluoropropyl fragment could be assigned with certainty because of peak overlap. ^{19}F NMR (282 MHz, CH_2Cl_2 with C_6D_6 capillary) δ -115.1 (d, $^2J_{\text{FF}} = 282$

Hz, 1F, $\text{Co}-\text{CF}_2\text{CF}_2\text{CF}_3$), -116.8 (d, $^2J_{\text{FF}} = 282$ Hz, 1F, $\text{Co}-\text{CF}_2\text{CF}_2\text{CF}_3$). MS [ESI (positive mode), solvent: MeOH] Calcd m/z (% intensity) for $[\text{CpCo}(\text{CF}_2\text{CF}_2\text{CF}_3)(\text{PPh}_2\text{Me})]^+$: 493.04 (100), 494.04 (23), 495.05 (3). Found: 493.04 (100), 494.04 (24). Calcd m/z (% intensity) for $[\text{CF}_3\text{CF}_2\text{CF}_2]^+$: 168.99 (100), 169.99 (3). Found: 168.99 (100), 169.99 (3).

$[\text{CpCo}(\text{CF}_3)(\text{CO})(\text{PPh}_2\text{Me})][\text{FB}(\text{C}_6\text{F}_5)_3]$ (**from Int 3**). Yield: 60% based on $\text{CpCo}(\text{CF}_3)_2(\text{PPh}_2\text{Me})$ after 4 h. ^{19}F NMR (282 MHz, CH_2Cl_2 with C_6D_6 capillary) δ 12.1 (d, $^3J_{\text{FF}} = 4$ Hz, 3F, $\text{Co}-\text{CF}_3$). $^{31}\text{P}\{^1\text{H}\}$ NMR (121 MHz, CH_2Cl_2 with C_6D_6 capillary) δ 33.0 (br, $\omega_{1/2} \approx 60$ Hz).

$\text{CpCo}(\text{CF}_2\text{CF}_3)(\text{FB}(\text{C}_6\text{F}_5)_3)(\text{PPh}_2\text{Me})$ (**from Int 3**). Yield: 35% based on $\text{CpCo}(\text{CF}_3)_2(\text{PPh}_2\text{Me})$ after 4 h. ^{19}F NMR (282 MHz, CH_2Cl_2 with C_6D_6 capillary) δ -76.7 (dd, $^2J_{\text{FF}} \approx 251$ Hz, $^3J_{\text{FF}} \approx 14$ Hz, 1F, $\text{CF}^{\text{A}}\text{F}^{\text{A}'}; \text{F}^{\text{A}}$), -80.5 (br, 3F, $\text{Co}-\text{CF}_2\text{CF}_3$), -86.6 (dd, $^2J_{\text{FF}} \approx 251$ Hz, $^3J_{\text{FF}} \approx 35$ Hz 1F, $\text{CF}^{\text{A}}\text{F}^{\text{A}'}; \text{F}^{\text{A}}$). $^{31}\text{P}\{^1\text{H}\}$ NMR (121 MHz, CH_2Cl_2 with C_6D_6 capillary) δ 25.2 (br, $\omega_{1/2} \approx 96$ Hz).

$[\text{CpCo}(\text{CF}_2\text{CF}_3)(\text{CO})(\text{PPh}_2\text{Me})][\text{FB}(\text{C}_6\text{F}_5)_3]$ (**from Int 4**). Yield and NMR assignments could not be obtained because of peak overlap.

$\text{CpCo}(\text{CF}_2\text{CF}_2\text{CF}_3)(\text{FB}(\text{C}_6\text{F}_5)_3)(\text{PPh}_2\text{Me})$ (**from Int 4**). Yield: 10% based on $\text{Co}-\text{CF}_2\text{CF}_2\text{CF}_3$ after 24 h. Only the F_β signals of the perfluoropropyl fragment could be assigned with certainty because of peak overlap. ^{19}F NMR (282 MHz, CH_2Cl_2 with C_6D_6 capillary) δ -112.6 (d, $^2J_{\text{FF}} = 284$ Hz, 1F, $\text{Co}-\text{CF}_2\text{CF}_2\text{CF}_3$), -114.3 (d, $^2J_{\text{FF}} = 284$ Hz, 1F, $\text{Co}-\text{CF}_2\text{CF}_2\text{CF}_3$).

General Procedure for the Catalytic Formation of *p*-Toluoyl Fluoride. The formation of *p*-toluoyl fluoride could be easily established by the growth of a sharp singlet at $\delta(^{19}\text{F}) = 16.5$ ppm. The only other signals observed via ^{19}F NMR were a mixture of $\text{CpCo}(\text{CF}_3)(\text{Cl})(\text{PPh}_2\text{Me})$ and $\text{CpCo}(\text{CF}_3)(\text{F})(\text{PPh}_2\text{Me})$ (**6**). Yields for the formation of the target compound were established by integration to BTB. See Table 1 for yields and selected control experiments and Table S16 for a full list.

Control Reactions with Various Fluoride Sources. To 0.8 mL of DCM in a vial was added AgF (92 mg, 0.72 mmol), CsF (110 mg, 0.72 mmol), KF (42 mg, 0.72 mmol), or CoF_3 (84 mg, 0.72 mmol). To this suspension were added *p*-toluoyl chloride (32 μL , 0.24 mmol) and BTB (18.6 μL , 0.12 mmol). The reaction was stirred vigorously (in the absence of light in the case of AgF) for 16 h and then transferred to an NMR tube with a C_6D_6 capillary.

Catalytic Reactions with Varying Catalyst Loadings. A stock solution (0.0152 M) was prepared for the reactions involving **5**, **1**, and **0.1 mol %** $\text{CpCo}(\text{CF}_3)(\text{I})(\text{PPh}_2\text{Me})$ (**2**). The complex (40 mg, 0.076 mmol) was dissolved in DCM (5 mL), affording a dark-yellow-brown solution.

10 mol % Loading. $\text{CpCo}(\text{CF}_3)(\text{I})(\text{PPh}_2\text{Me})$ (**2**) (13 mg, 0.024 mmol) was added to a vial, along with AgF (92 mg, 0.72 mmol) and DCM (0.8 mL). To this dark-yellow-brown solution were added *p*-toluoyl chloride (32 μL , 0.24 mmol) and BTB (18.6 μL , 0.12 mmol). The reaction was stirred vigorously (in the absence of light) for 4 h and then transferred to an NMR with a C_6D_6 capillary.

5 mol % Loading. $\text{CpCo}(\text{CF}_3)(\text{I})(\text{PPh}_2\text{Me})$ (**2**) (0.79 mL, 0.012 mmol) was added to a vial, along with AgF (92 mg, 0.72 mmol). To this dark-yellow-brown solution were added *p*-toluoyl chloride (32 μL , 0.24 mmol) and BTB (18.6 μL , 0.12 mmol). The reaction was stirred vigorously (in the absence of light) for 4 h and then transferred to an NMR with a C_6D_6 capillary.

1 mol % Loading. $\text{CpCo}(\text{CF}_3)(\text{I})(\text{PPh}_2\text{Me})$ (**2**) (0.16 mL, 0.0024 mmol) was added to a vial, along with AgF (92 mg, 0.72 mmol) and DCM (0.64 mL). To this pale-yellow-brown solution were added *p*-toluoyl chloride (32 μL , 0.24 mmol) and BTB (18.6 μL , 0.12 mmol). The reaction was stirred vigorously (in the absence of light) for 4 h and then transferred to an NMR with a C_6D_6 capillary.

0.1 mol % Loading. To 0.8 mL of DCM in a vial was added $\text{CpCo}(\text{CF}_3)(\text{I})(\text{PPh}_2\text{Me})$ (**2**) (79 μL , 0.0012 mmol) and AgF (92 mg, 0.72 mmol). To this pale-yellow-brown solution were added *p*-toluoyl chloride (32 μL , 0.24 mmol) and BTB (18.6 μL , 0.12 mmol). The reaction was stirred vigorously (in the absence of light) for 4 h and then transferred to an NMR with a C_6D_6 capillary.

■ ASSOCIATED CONTENT

■ Supporting Information

The Supporting Information is available free of charge on the ACS Publications website at DOI: 10.1021/jacs.5b12003.

Experimental details, TD-DFT and frontier orbital studies, details of NMR calculations and results, optimized Cartesian coordinates in Å, ^1H , ^{19}F and $^{31}\text{P}\{^1\text{H}\}$ NMR spectra, IR spectra, and powder X-ray diffraction data. (PDF)

Crystallographic information file for compound 5. (CIF)

Crystallographic information file for compound 6. (CIF)

Crystallographic information file for compound 7. (CIF)

Crystallographic information file for compound 8. (CIF)

Crystallographic information file for compound 9. (CIF)

Crystallographic information file for compound 10. (CIF)

■ AUTHOR INFORMATION

Corresponding Author

*rbaker@uottawa.ca

Notes

The authors declare no competing financial interest.

■ ACKNOWLEDGMENTS

We thank the NSERC and the Canada Research Chairs program for generous financial support and the University of Ottawa, Canada Foundation for Innovation, and Ontario Ministry of Economic Development and Innovation for essential infrastructure. Dr. Glenn Facey is thanked for helpful discussions and assistance with NMR experiments. Rebecca Holmberg is thanked for PXRD experiments. M.C.L., J.M.B., and G.M.L. gratefully acknowledge support from NSERC. A portion of the computational work was supported by the Chemical Sciences, Geosciences and Biosciences Division, Office of Basic Energy Sciences, U.S. Department of Energy (DOE) (catalysis center program). D.A.D. also thanks the Robert Ramsay Chair Fund of The University of Alabama for support.

■ REFERENCES

- (1) Murphy, E. F.; Murugavel, R.; Roesky, H. W. *Chem. Rev.* **1997**, *97*, 3425–3468.
- (2) Taw, F. L.; Clark, A. E.; Mueller, A. H.; Janicke, M. T.; Cantat, T.; Scott, B. L.; Hay, P. J.; Hughes, R. P.; Kiplinger, J. L. *Organometallics* **2012**, *31*, 1484–1499.
- (3) (a) Emelús, H. J.; Haszeldine, R. N. *J. Chem. Soc.* **1949**, 2953–2956. (b) Martínez-Salvador, S.; Falvello, L. R.; Martín, A.; Menjón, B. *Chem. - Eur. J.* **2013**, *19*, 14540–14552. (c) Blaya, M.; Bautista, D.; Gil-Rubio, J.; Vicente, J. *Organometallics* **2014**, *33*, 6358–6368. (d) Burton, D. J.; Wiemers, D. M. *J. Am. Chem. Soc.* **1985**, *107*, 5014–5015.
- (4) (a) Yamaguchi, Y.; Ichioka, H.; Klein, A.; Brennessel, W. W.; Vicić, D. A. *Organometallics* **2012**, *31*, 1477–1483. (b) Tang, F.; Rath, N. P.; Mirica, L. M. *Chem. Commun.* **2015**, *51*, 3113–3116. (c) Bour, J. R.; Camasso, N. M.; Sanford, M. S. *J. Am. Chem. Soc.* **2015**, *137*, 8034–8037.
- (5) (a) Bourgeois, C. J.; Hughes, R. P.; Husebo, T. L.; Smith, J. M.; Guzei, I. M.; Liable-Sands, L. M.; Zakharov, L. N.; Rheingold, A. L. *Organometallics* **2005**, *24*, 6431–6439. (b) Hughes, R. P.; Lindner, D. C.; Smith, J. M.; Zhang, D.; Incarvito, C. D.; Lam, K.-C.; Liable-Sands, L. M.; Sommer, R. D.; Rheingold, A. L. *J. Chem. Soc., Dalton Trans.* **2001**, *15*, 2270–2278.
- (6) (a) Tomashenko, O. A.; Grushin, V. V. *Chem. Rev.* **2011**, *111*, 4475–4521. (b) Bourgeois, C. J.; Garratt, S. A.; Hughes, R. P.; Larichev, R. B.; Smith, J. M.; Ward, A. J.; Willemsen, S.; Zhang, D.; DiPasquale, A. G.; Zakharov, L. N.; Rheingold, A. L. *Organometallics* **2006**, *25*, 3474–3480.
- (7) (a) Taw, F. L.; Scott, B. L.; Kiplinger, J. L. *J. Am. Chem. Soc.* **2003**, *125*, 14712–14713. (b) Vabre, B.; Petiot, P.; Declercq, R.; Zargarian, D. *Organometallics* **2014**, *33*, 5173–5184. (c) Liu, X.; Xu, C.; Wang, M.; Liu, Q. *Chem. Rev.* **2014**, *115*, 683. (d) Huang, D.; Caulton, K. G. *J. Am. Chem. Soc.* **1997**, *119*, 3185–3186. (e) Vicente, J.; Gil-Rubio, J.; Guerrero-Leal, J.; Bautista, D. *Organometallics* **2004**, *23*, 4871–4881.
- (8) King, R. B.; Treichel, P. M.; Stone, F. G. A. *J. Am. Chem. Soc.* **1961**, *83*, 3593–3597.
- (9) Burns, R. J.; Bulkowski, P. B.; Stevens, S. C. V.; Baird, M. C. J. *Chem. Soc., Dalton Trans.* **1974**, *4*, 415–420.
- (10) (a) Harrison, D. J.; Gorelsky, S. I.; Lee, G. M.; Korobkov, I.; Baker, R. T. *Organometallics* **2013**, *32*, 12–15. (b) Harrison, D. J.; Lee, G. M.; Leclerc, M. C.; Korobkov, I.; Baker, R. T. *J. Am. Chem. Soc.* **2013**, *135*, 18296–18299.
- (11) Parr, R. G.; Yang, W. In *Density-Functional Theory of Atoms and Molecules*; Oxford University Press: New York, 1989.
- (12) Becke, A. D. *J. Chem. Phys.* **1993**, *98*, 5648–5652.
- (13) Lee, C.; Yang, W.; Parr, R. G. *Phys. Rev. B: Condens. Matter Mater. Phys.* **1988**, *37*, 785–789.
- (14) Perdew, J. P.; Wang, Y. *Phys. Rev. B: Condens. Matter Mater. Phys.* **1992**, *45*, 13244–13249.
- (15) Burke, K.; Perdew, J. P.; Wang, Y. In *Electronic Density Functional Theory: Recent Progress and New Directions*; Dobson, J. F., Vignale, G., Das, M. P., Eds.; Plenum: New York, 1998.
- (16) (a) Dugan, T. R.; Sun, X.; Rybak-Akimova, E. V.; Olatunji-Ojo, O.; Cundari, T. R.; Holland, P. L. *J. Am. Chem. Soc.* **2011**, *133*, 12418–12421. (b) Dugan, T. R.; Goldberg, J. M.; Brennessel, W. W.; Holland, P. L. *Organometallics* **2012**, *31*, 1349–1360.
- (17) Li, X.; Sun, H.; Yu, F.; Flörke, U.; Klein, H.-F. *Organometallics* **2006**, *25*, 4695–4697.
- (18) Bennett, B. K.; Harrison, R. G.; Richmond, T. G. *J. Am. Chem. Soc.* **1994**, *116*, 11165–11166.
- (19) (a) Ketelaar, J. J. *Nature* **1931**, *128*, 303. (b) Hepworth, M. A.; Jack, K. H.; Peacock, R. D.; Westland, G. J. *Acta Crystallogr.* **1957**, *10*, 63–69.
- (20) Treichel, P. M.; Stone, F. G. A. *Adv. Organomet. Chem.* **1964**, *1*, 143–220.
- (21) Zhang, C.-P.; Wang, H.; Klein, A.; Biewer, C.; Stirnat, K.; Yamaguchi, Y.; Xu, L.; Gomez-Benitez, V.; Vicić, D. A. *J. Am. Chem. Soc.* **2013**, *135*, 8141–8144.
- (22) Marenich, A. V.; Cramer, C. J.; Truhlar, D. G. *J. Phys. Chem. B* **2009**, *113*, 6378–6396.
- (23) Lever, A. B. P. In *Inorganic Electronic Spectroscopy*; Elsevier: Amsterdam, 1984.
- (24) Mayer, I. *Theor. Chim. Acta* **1985**, *67*, 315–322.
- (25) Veltheer, J. E.; Burger, P.; Bergman, R. G. *J. Am. Chem. Soc.* **1995**, *117*, 12478–12488.
- (26) (a) Wiberg, K. B.; Hammer, J. D.; Zilm, K. W.; Cheeseman, J. R.; Keith, T. A. *J. Phys. Chem. A* **1998**, *102*, 8766–8773. (b) Alexakos, L. G.; Cornwell, C. D. *J. Chem. Phys.* **1964**, *41*, 2098–2107. (c) Cornwell, C. D. *J. Chem. Phys.* **1966**, *44*, 874–880.
- (27) Ahrens, T.; Kohlmann, J.; Ahrens, M.; Braun, T. *Chem. Rev.* **2015**, *115*, 931–972.
- (28) Champagne, P. A.; Desroches, J.; Hamel, J.-D.; Vandamme, M.; Paquin, J.-F. *Chem. Rev.* **2015**, *115*, 9073.
- (29) Maity, A.; Stanek, R. J.; Anderson, B. L.; Zeller, M.; Hunter, A. D.; Moore, C. E.; Rheingold, A. L.; Gray, T. G. *Organometallics* **2015**, *34*, 109–120.
- (30) Birrell, J. A.; Desrosiers, J.-N.; Jacobsen, E. N. *J. Am. Chem. Soc.* **2011**, *133*, 13872–13875.
- (31) Stavber, S.; Košir, I.; Zupan, M. *J. Org. Chem.* **1997**, *62*, 4916–4920.
- (32) Motie, R. E.; Satchell, D. P. N.; Wassef, W. N. *J. Chem. Soc., Perkin Trans. 2* **1993**, *6*, 1087–1090.
- (33) Lee, I.; Shim, C. S.; Chung, S. Y.; Kim, H. Y.; Lee, H. W. *J. Chem. Soc., Perkin Trans. 2* **1988**, *11*, 1919–1923.

- (34) Okano, T.; Harada, N.; Kiji, J. *Bull. Chem. Soc. Jpn.* **1992**, *65*, 1741–1743.
- (35) Campbell, M. G.; Ritter, T. *Chem. Rev.* **2015**, *115*, 612–633.
- (36) Hollingworth, C.; Gouverneur, V. *Chem. Commun.* **2012**, *48*, 2929–2942.
- (37) (a) Mankad, N. P.; Toste, F. D. *Chem. Sci.* **2012**, *3*, 72–76. (b) Hull, K. L.; Anani, W. Q.; Sanford, M. S. *J. Am. Chem. Soc.* **2006**, *128*, 7134–7135. (c) Racowski, J. M.; Gary, J. B.; Sanford, M. S. *Angew. Chem., Int. Ed.* **2012**, *51*, 3414–3417.
- (38) (a) Akana, J. A.; Bhattacharyya, K. X.; Müller, P.; Sadighi, J. P. *J. Am. Chem. Soc.* **2007**, *129*, 7736–7737. (b) Gorske, B. C.; Mbofana, C. T.; Miller, S. J. *Org. Lett.* **2009**, *11*, 4318–4321. (c) Schuler, M.; Silva, F.; Bobbio, C.; Tessier, A.; Gouverneur, V. *Angew. Chem., Int. Ed.* **2008**, *47*, 7927–7930.
- (39) (a) Ball, N. D.; Sanford, M. S. *J. Am. Chem. Soc.* **2009**, *131*, 3796–3797. (b) Zhao, S.-B.; Wang, R.-Y.; Nguyen, H.; Becker, J. J.; Gagné, M. R. *Chem. Commun.* **2012**, *48*, 443–445. (c) Furuya, T.; Strom, A. E.; Ritter, T. *J. Am. Chem. Soc.* **2009**, *131*, 1662–1663. (d) Furuya, T.; Ritter, T. *Org. Lett.* **2009**, *11*, 2860–2863. (e) Tang, P.; Ritter, T. *Tetrahedron* **2011**, *67*, 4449–4454.
- (40) (a) Fier, P. S.; Hartwig, J. F. *J. Am. Chem. Soc.* **2012**, *134*, 10795–10798. (b) Mu, X.; Liu, G. *Org. Chem. Front.* **2014**, *1*, 430–433. (c) Casitas, A.; Canta, M.; Solà, M.; Costas, M.; Ribas, X. *J. Am. Chem. Soc.* **2011**, *133*, 19386–19392.
- (41) (a) Grushin, V. V. *Acc. Chem. Res.* **2010**, *43*, 160–171. (b) Grushin, V. V. *Chem. - Eur. J.* **2002**, *8*, 1006–1014. (c) Macgregor, S. A.; Roe, D. C.; Marshall, W. J.; Bloch, K. M.; Bakhmutov, V. I.; Grushin, V. V. *J. Am. Chem. Soc.* **2005**, *127*, 15304–15321.
- (42) (a) Wang, X.; Mei, T.-S.; Yu, J.-Q. *J. Am. Chem. Soc.* **2009**, *131*, 7520–7521. (b) Chan, K. S. L.; Wasa, M.; Wang, X.; Yu, J.-Q. *Angew. Chem., Int. Ed.* **2011**, *50*, 9081–9084.
- (43) Doherty, N. M.; Hoffmann, N. W. *Chem. Rev.* **1991**, *91*, 553–573.
- (44) Urata, H.; Fuchikami, T. *Tetrahedron Lett.* **1991**, *32*, 91–94.
- (45) Maggiora, W.; Tyrre, D.; Naumann, N.; Kirij, V.; Yagupolskii, Y. L. *Angew. Chem., Int. Ed.* **1999**, *38*, 2252–2253.
- (46) Kolomeitsev, A.; Movchun, V.; Rusanov, E.; Bissky, G.; Lork, E.; Röschenhaler, G.-V.; Kirsch, P. *Chem. Commun.* **1999**, 1017–1018.
- (47) Wang, X.; Xu, Y.; Mo, F.; Ji, G.; Qiu, D.; Feng, J.; Ye, Y.; Zhang, S.; Zhang, Y.; Wang, J. *J. Am. Chem. Soc.* **2013**, *135*, 10330–10333.
- (48) Combettes, L. E.; Clausen-Thue, P.; King, M. A.; Odell, B.; Thompson, A. L.; Gouverneur, V.; Claridge, T. D. W. *Chem. - Eur. J.* **2012**, *18*, 13133–13141.
- (49) Clark, G. R.; Hoskins, S. V.; Jones, T. C.; Roper, W. R. *J. Chem. Soc., Chem. Commun.* **1983**, 719–721.
- (50) For other examples of d_6 metal difluorocarbene ^{19}F NMR shifts, see (a) Richmond, T. G.; Crespi, A. M.; Shriver, D. W. *Organometallics* **1984**, *3*, 314–319. (b) Trnka, T. M.; Day, M. W.; Grubbs, R. H. *Angew. Chem., Int. Ed.* **2001**, *40*, 3441–3444.
- (51) Jablonski, C. R.; Zhou, Z. *Can. J. Chem.* **1992**, *70*, 2544–2551.
- (52) (a) Wiemers, D. M.; Burton, D. J. *J. Am. Chem. Soc.* **1986**, *108*, 832–834. (b) Yang, Z. Y.; Wiemers, D. M.; Burton, D. J. *J. Am. Chem. Soc.* **1992**, *114*, 4402–4403.
- (53) Wilford, J. B.; Stone, F. G. A. *Inorg. Chem.* **1965**, *4*, 93–97.
- (54) Dichloromethane was used as a solvent because it is not hygroscopic and because it is one of the easiest to dry to minimal water content. For more information pertaining to the drying of various solvents, see Williams, D. B. G.; Lawton, M. J. *Org. Chem.* **2010**, *75*, 8351–8354.
- (55) Brothers, P. J.; Roper, W. R. *Chem. Rev.* **1988**, *88*, 1293–1326.